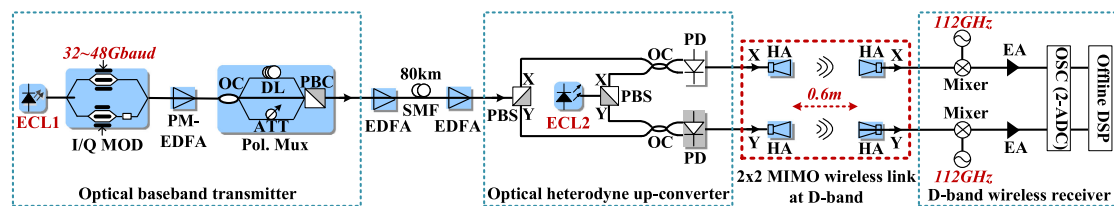


# Over 100 Gb/s Ultrabroadband MIMO Wireless Signal Delivery System at the D-Band

Volume 8, Number 5, October 2016

Xinying Li  
Jianjun Yu



DOI: 10.1109/JPHOT.2016.2601780  
1943-0655 © 2016 IEEE

# Over 100 Gb/s Ultrabroadband MIMO Wireless Signal Delivery System at the D-Band

Xinying Li<sup>1,2</sup> and Jianjun Yu<sup>1,2</sup>

<sup>1</sup>Department of Communication Science and Engineering and Key Laboratory for Information Science of Electromagnetic Waves (MoE), Fudan University, Shanghai 200433, China

<sup>2</sup>ZTE (TX) Inc., Morristown, NJ 07920 USA

DOI:10.1109/JPHOT.2016.2601780

1943-0655 © 2016 IEEE. Translations and content mining are permitted for academic research only.  
Personal use is also permitted, but republication/redistribution requires IEEE permission.  
See [http://www.ieee.org/publications\\_standards/publications/rights/index.html](http://www.ieee.org/publications_standards/publications/rights/index.html) for more information.

Manuscript received June 20, 2016; revised August 15, 2016; accepted August 17, 2016. Date of publication August 19, 2016; date of current version September 9, 2016. This work was supported in part by the NNSF of China (61325002, 61250018, 61527801), the National High-tech R&D Program (863 Program) of China (2015AA016904), Key Program of Shanghai Science and Technology Association (13JC1400700), and the Ph.D. Programs Foundation of the Ministry of Education of China (20120071110032). Corresponding author: Xinying Li (e-mail: xinying.li@ece.gatech.edu).

**Abstract:** We propose and experimentally demonstrate an ultrabroadband wireless millimeter-wave (mm-wave) signal delivery system at the D-band (110–170 GHz), employing the techniques of photonics-aided mm-wave generation, wireless multiple-input multiple-output (MIMO), and high-level vector signal modulation, combined with digital heterodyne coherent detection. Our demonstrated system not only can deliver up to 46-Gbaud (184-Gbit/s) polarization-division-multiplexing quadrature-phase-shift-keying (PDM-QPSK) signal over 80-km single-mode fiber-28 (SMF-28) and 0.6-m 2 × 2 MIMO wireless link at the D-band but can deliver up to a 16-Gbaud (128-Gbit/s) polarization-division-multiplexing 16-ary quadrature-amplitude-modulation (PDM-16QAM) signal over 10-cm 2 × 2 MIMO wireless link at the D-band as well. To the best of our knowledge, we have realized a record bit rate of 184 Gbit/s for the D-band wireless mm-wave signal delivery.

**Index Terms:** D-band, multiple-input multiple-output (MIMO), photonics-aided millimeter-wave (mm-wave) generation, vector signal modulation.

## 1. Introduction

High-speed broadband wireless communications have been widely used in mobile telephone, wireless local area networks (WLANs), satellite communication, and other consumer electronic equipment. Millimeter-wave (mm-wave) band (30 GHz–300 GHz) and terahertz-wave band (300 GHz–10 THz) have sufficient bandwidth to accommodate wideband signal and may be the location of future Gb/s-class broadband wireless communication systems [1]–[9]. However, it is difficult to generate high-speed/high-carrier-frequency wireless mm-wave signals simply based on electrical techniques because of the bandwidth limitation of state-of-the-art electronic devices. Photonics-aided mm-wave generation techniques, which are basically based on the heterodyne beating of two continuous-wave (CW) lightwaves spaced by a desired mm-wave carrier frequency, can overcome the bottleneck bandwidth of electronic devices and realize high-speed/high-carrier-frequency wireless mm-wave signal generation with a relatively low cost and simple architecture [10]–[12]. Moreover, photonics-aided mm-wave generation techniques can seamlessly integrate with various

kinds of advanced techniques, particularly wireless multiple-input multiple-output (MIMO) [13]–[19] and vector signal modulation combined with digital heterodyne coherent detection [20]–[27], to increase wireless transmission capacity, which have been intensively studied and widely demonstrated by the research community.

The technique of wireless MIMO [13]–[19] employs two pairs of antennas, and can realize wireless delivery of two wireless mm-wave signals. Therefore, this technique can effectively reduce signal baud rate and the bandwidth demand of electro-optic devices, and increase the wireless transmission capacity. The technique of vector signal modulation combined with digital heterodyne coherent detection [20]–[27] not only can make full use of various kinds of advanced high-level modulation formats, such as quadrature-phase-shift-keying (QPSK), 16-ary quadrature-amplitude-modulation (16QAM), 64QAM, and so on, to improve device's bandwidth efficiency and system's spectral efficiency, but also can make full use of existing digital coherent algorithms to effectively compensate for various kinds of linear/nonlinear component impairments and transmission impairments and improve receiver sensitivity. Therefore, this technique can also effectively increase the wireless transmission capacity.

Recently, 100-Gb/s and beyond wireless transmission rates have been attained at W-band (75 GHz–110 GHz) based on the aforementioned various kinds of advanced techniques [15]–[20], [23]. However, in previous W-band experimental demonstrations, the attained highest wireless transmission baud rate is 27 Gbaud [16], [17]. Compared to W-band, D-band (110 GHz–170 GHz) has larger available bandwidth to attain higher wireless transmission baud rate while maintaining a relatively low atmospheric and rain loss. However, until now, not too much research has been reported on D-band wireless mm-wave delivery. Moreover, the reported wireless transmission links at D-band are typically single-input single-output (SISO) and have relatively low wireless transmission rates (no more than 60 Gb/s) [28]–[32]. Very recently, we have experimentally demonstrated for the first time a  $2 \times 2$  MIMO wireless mm-wave signal delivery system at D-band [33]. However, only 8-Gbaud wireless mm-wave signal delivery is attained in this experimental demonstration because of the lack of sufficient-bandwidth mm-wave components.

In this paper, we propose and experimentally demonstrate an ultra-broadband wireless mm-wave signal delivery system at D-band, employing the techniques of photonics-aided mm-wave generation, wireless MIMO, and high-level vector signal modulation combined with digital heterodyne coherent detection. Our demonstrated system not only can deliver up to 46-Gbaud (184-Gb/s) polarization-division-multiplexing QPSK (PDM-QPSK) signal over 80-km single-mode fiber-28 (SMF-28) and 0.6-m  $2 \times 2$  MIMO wireless link at D-band, but also can deliver up to 16-Gbaud (128-Gb/s) polarization-division-multiplexing 16QAM (PDM-16QAM) signal over 10-cm  $2 \times 2$  MIMO wireless link at D-band. The bit-error ratio (BER) is under the soft-defined forward-error-correction (SD-FEC) threshold of  $2 \times 10^{-2}$ . After removing 20% SD-FEC threshold, the net bit rates for the PDM-QPSK and PDM-16QAM cases are  $184/(1 + 20\%) = 153.3$  Gb/s and  $128/(1 + 20\%) = 106.7$  Gb/s, respectively. To the best of our knowledge, we realize a record bit rate of 184 Gb/s for D-band wireless mm-wave signal delivery. We think our work described in the paper offers a powerful proof for wireless mm-wave signal delivery system located at D-band to be a promising candidate of the future broadband wireless communications.

## 2. Experimental Setup for Ultra-Broadband Photonics-aided D-Band MIMO Wireless mm-Wave Signal Delivery System

Fig. 1 shows the experimental setup for the ultra-broadband photonics-aided D-band MIMO wireless mm-wave signal delivery system. Two free-running external cavity lasers (ECLs), i.e., ECL1 and ECL2, are employed with less than 100-kHz linewidth and 13-dBm output power. At the optical baseband transmitter, the CW lightwave from ECL1 at 1551.37-nm operating wavelength is modulated by a 32~48-Gbaud electrical binary signal via an in-phase/quadrature (I/Q) modulator. The 32~48-Gbaud electrical binary signal with a pseudo-random binary sequence (PRBS) length of  $2^{15} - 1$  is offered by an 80-GSa/s digital-to-analog converter (DAC) with a 16-GHz 3-dB electrical bandwidth. The I/Q modulator has a 31-GHz 3-dB optical bandwidth and a 2.5-V half-wave

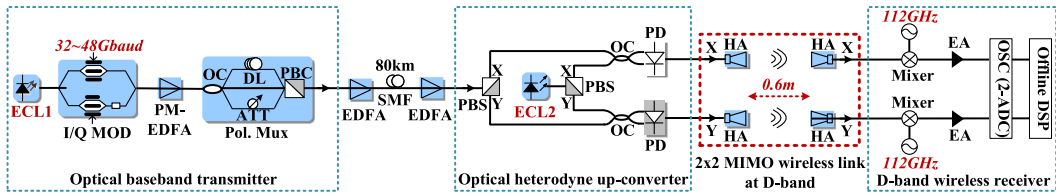


Fig. 1. Experimental setup for the ultra-broadband photonics-aided D-band MIMO wireless mm-wave signal delivery system. ECL: external cavity laser, I/Q MOD: I/Q modulator, PM-EDFA: polarization-maintaining erbium-doped fiber amplifier, OC: optical coupler, DL: optical delay line, ATT: optical attenuator, PBC: polarization beam combiner, Pol. Mux.: polarization multiplexer, SMF: single-mode fiber, PBS: polarization beam splitter, PD: photodiode, HA: horn antenna, EA: electrical amplifier, OSC: oscilloscope, DSP: digital signal processing.

voltage at 1 GHz. The two parallel Mach-Zehnder modulators (MZMs) in the I/Q modulator are both biased at the null point and driven at the full swing, while the upper and lower branches of the I/Q modulator has a fixed  $\pi/2$  phase difference, in order to convert the electrical binary signal into an optical QPSK signal centered at 1551.37 nm. The generated optical QPSK signal is boost by a polarization-maintaining erbium-doped fiber amplifier (PM-EDFA), and then polarization multiplexed by a polarization multiplexer, to generate an optical PDM-QPSK signal. The polarization multiplexer comprises a polarization-maintaining optical coupler (OC) to split the input optical QPSK signal into two tributaries, an optical delay line (DL) in one arm to provide a 150-symbol delay, an optical attenuator in the other arm to balance the power of the two tributaries, and a polarization beam combiner (PBC) to recombine the two tributaries into an optical PDM-QPSK signal. After boost by an erbium-doped fiber amplifier (EDFA), the generated optical PDM-QPSK signal with 6-dBm optical power is launched into 80-km SMF-28, which has 18-dB average loss and 17-ps/km/nm chromatic dispersion (CD) at 1550 nm without optical dispersion compensation.

Next, after boost by another EDFA, the received optical PDM-QPSK signal is sent into an optical polarization-diversity heterodyne up-converter [16], in which ECL2 is used as an optical local oscillator (LO) source and has a 137.5-GHz frequency spacing relative to ECL1. It is worth noting that the frequency spacing between ECL1 and ECL2 are adjustable and can be located at any D-band frequency in our experiment. Two polarization beam splitters (PBSs) and two OCs implement optical polarization-diversity splitting for the received optical PDM-QPSK signal and the optical LO source to attain X-polarization and Y-polarization optical components, which are then simultaneously up-converted by two parallel D-band single-ended photodiodes (PDs) into two QPSK modulated wireless mm-wave signals at 137.5 GHz. The two QPSK modulated wireless mm-wave signals can be considered as a PDM-QPSK modulated wireless mm-wave signal. It is worth noting that the polarization of the light in front of the PBS for splitting signal is arbitrary due to fiber transmission. Thus, the X- or Y-polarization component at the output port of the PBS contains a mix of the data which is simultaneously encoded on the X- and Y-polarization at the transmitter.

Fig. 2(a) gives the X-polarization optical spectrum after optical polarization-diversity splitting measured at 0.1-nm resolution and 32 Gbaud. Fig. 2(b)–(d) give the performance curves of the D-band single-ended PD. Fig. 2(b) gives the output power versus the DC bias for the D-band single-ended PD in the scenario of 140-GHz operating frequency and 7-mA output photocurrent. We can see that, when the DC bias varies within the range from  $-2.8$  V to  $-1.4$  V, the PD can have a relatively stable output power of about  $-7$  dBm. The DC bias of the D-band single-ended PD is fixed at  $-2$  V in our experiment. Fig. 2(c) gives the output power versus the output photocurrent for the D-band single-ended PD in the scenario of 140-GHz operating frequency and  $-2$ -V DC bias. We can see that the output power can be considered to be directly proportional to the output photocurrent. Fig. 2(d) gives the output power versus the operating frequency for the D-band single-ended PD in the scenario of  $-2$ -V DC bias and 7-mA output photocurrent. We can see that, within the whole D-band, the D-band PD has a relatively flat spectral response with a power fluctuation less than  $-3$  dB.

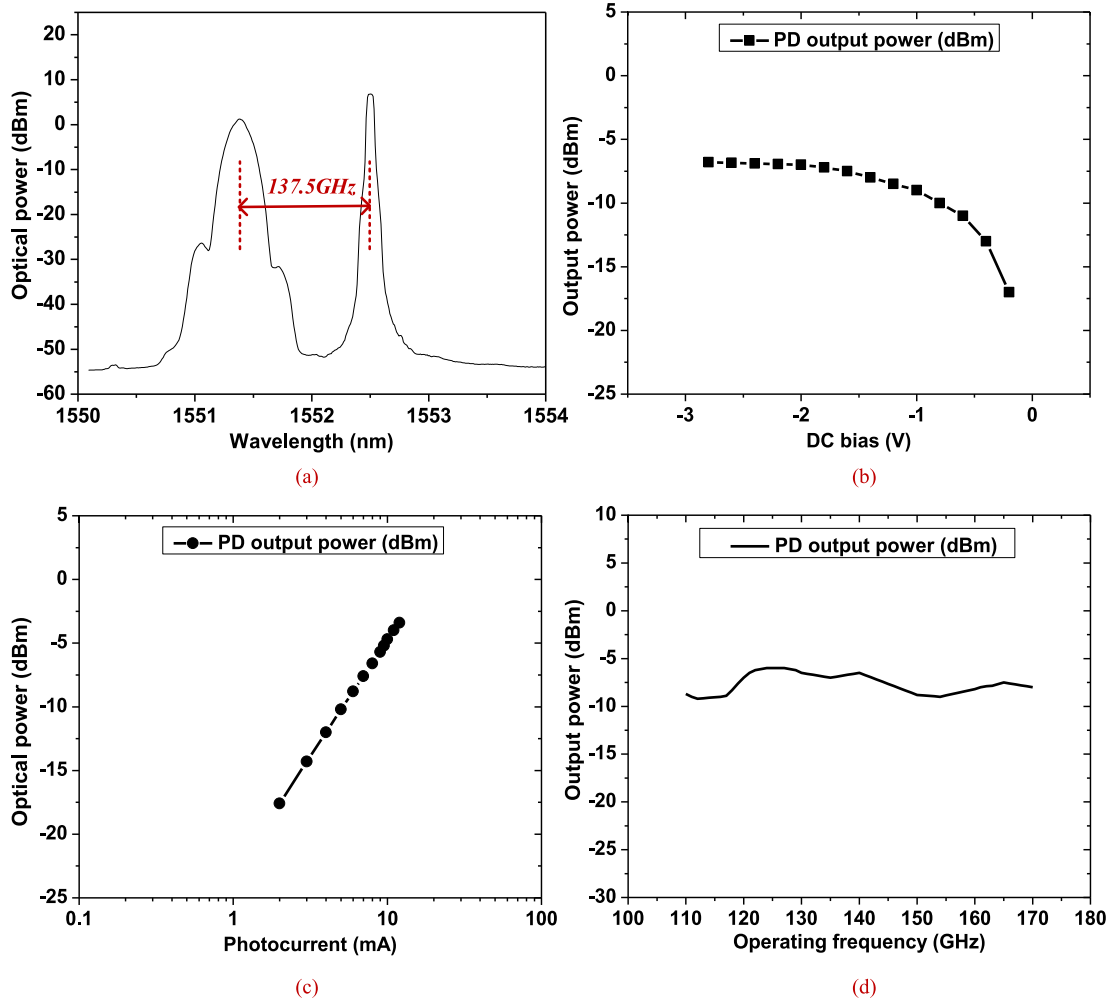


Fig. 2. Optical spectrum and performance curves of the D-band single-ended PD. (a) X-polarization optical spectrum after optical polarization-diversity splitting measured at 0.1-nm resolution and 32 Gbaud. (b) Output power versus the DC bias for the D-band single-ended PD in the scenario of 140-GHz operating frequency and 7-mA output photocurrent. (c) Output power versus the output photocurrent for the D-band single-ended PD in the scenario of 140-GHz operating frequency and -2-V DC bias. (d) Output power versus the operating frequency for the D-band single-ended PD in the scenario of -2-V DC bias and 7-mA output photocurrent.

Next, the generated PDM-QPSK modulated wireless mm-wave signal at 137.5 GHz is delivered over 0.6-m wireless distance by a  $2 \times 2$  multiple-input multiple-output (MIMO) wireless air link made up of two pairs of D-band horn antennas (HAs). The two transmitter (receiver) D-band HAs are separated by 0.4 m. Both good directionality as well as sufficient wireless separation between transmitter (receiver) D-band HAs ensures that no wireless crosstalk occurs between the X-polarization and Y-polarization wireless air links. Each D-band HA has a  $10^\circ$  3-dB beamwidth. Fig. 3(a) gives the gain of the D-band HA versus the operating frequency, and the D-band HA has an average gain of 25 dBi within the whole D-band. It is worth noting that the wireless transmitter power in our experiment is -12 dBm. According to the Friis transmission equation, we estimate the received power for a given wireless transmitter power  $P_T$  (equal to -12 dBm), transmitter/receiver antenna gain  $G_T/G_R$  (both equal to 25 dBi), and wireless transmission distance  $d$  (equal to 0.6 m). The received power  $P_R$  is given by

$$P_R(\text{dBm}) = P_T + G_T + G_R - 20 \log \left( \frac{4\pi d}{\lambda} \right) - L_F - L_A \times d \quad (1)$$

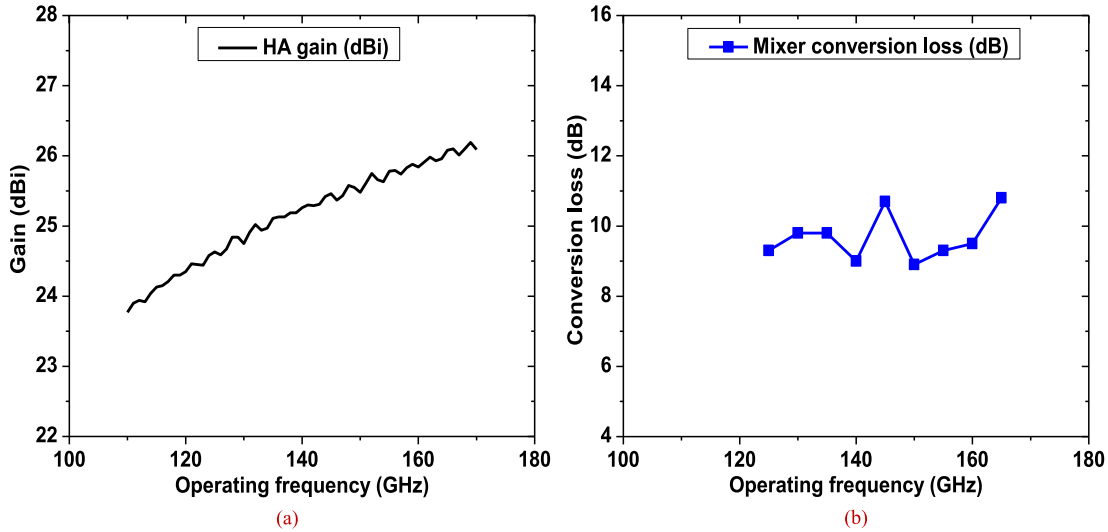


Fig. 3. Performance curves of the D-band single-ended HA and the D-band balanced mixer. (a) Gain of the D-band HA versus the operating frequency. (b) Conversion loss of the D-band balanced mixer versus the operating frequency in the scenario of 5-V DC bias.

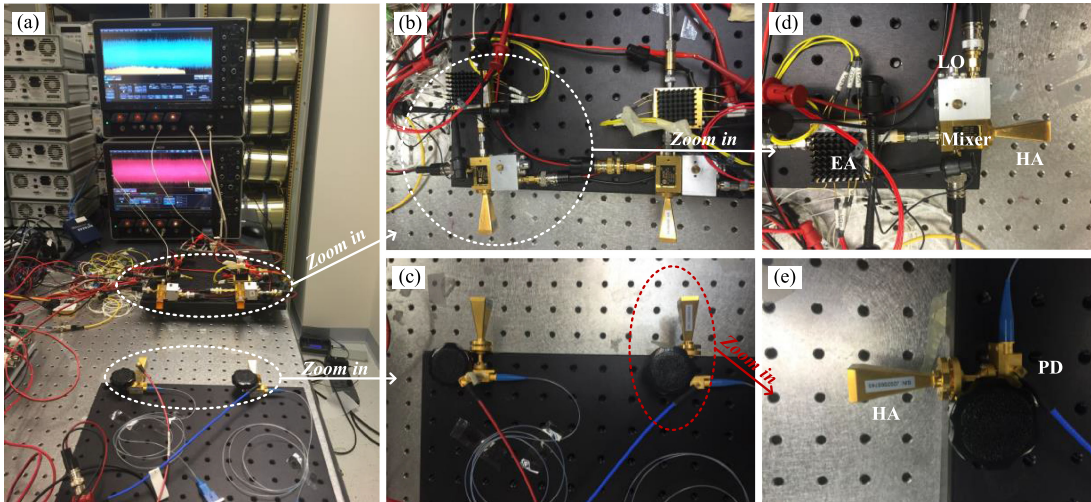


Fig. 4. (a) Whole wireless transmission link, (b) D-band wireless transmitter end, (c) D-band wireless receiver end, (d) X-polarization D-band wireless transmitter end, and (e) Y-polarization D-band wireless receiver end.

where  $\lambda$  denotes the wavelength spacing between the optical signal and the optical LO used for heterodyne beating and is equal to  $(\lambda_1^2 f_{RF})/c$ . Here,  $c$  denotes the velocity of light, and  $f_{RF}$  denotes the mm-wave carrier frequency.  $\lambda_1$  denotes the central wavelength of the optical signal, and it is equal to 1551.37 nm in our experiment. As a result,  $\lambda$  approximates 1.1 nm for 137.5-GHz mm-wave carrier frequency.  $L_F$  is the loss of antenna feedline and approximates 3 dB in our experiment.  $L_A$  is the atmospheric loss factor, and  $L_A$  at 137.5 GHz is about 0.9 dB/km on a sunny day [34]. The term  $20\log(4d\pi/\lambda)$  denotes the path loss. The atmospheric loss is about 0.54 dB and the path loss is about 98.36 dB for 0.6-m wireless mm-wave delivery. Therefore, the estimated received power is  $-63.9$  dBm for 0.6-m wireless mm-wave delivery at a 137.5-GHz center frequency.

At the D-band wireless mm-wave receiver, the received 137.5-GHz PDM-QPSK modulated wireless mm-wave signal is down-converted to a lower-frequency 25.5-GHz electrical mm-wave signal in the analog domain, with the aid of two parallel D-band balanced mixers and two sinusoidal

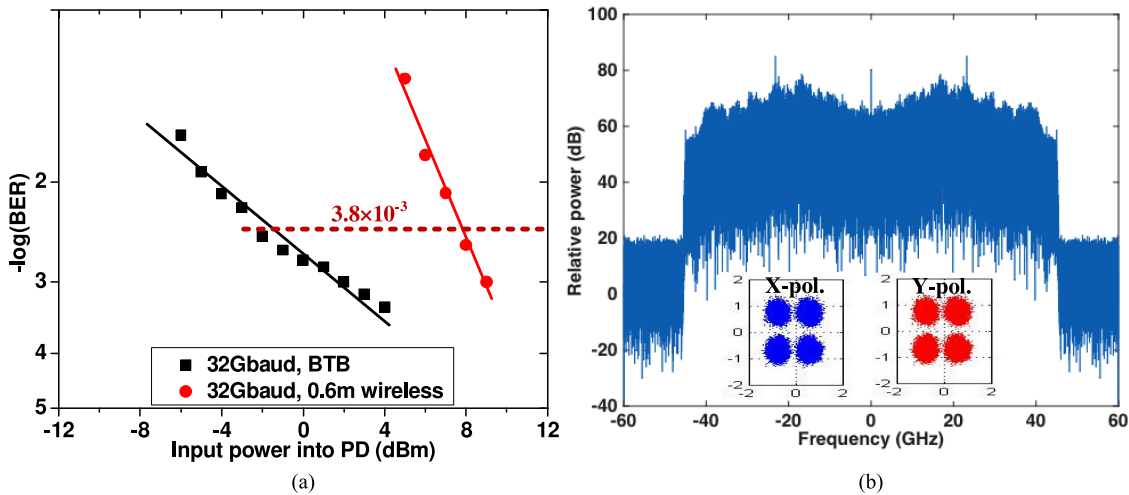


Fig. 5. (a) Measured BER performance versus the input power into each PD for the 32-Gbaud 137.5-GHz PDM-QPSK mm-wave signal after 80-km SMF-28 transmission in the scenario of no wireless delivery and 0.6-m wireless delivery, respectively. (b) and the two insets in (b) give the captured 25.5-GHz mm-wave signal spectrum, as well as the recovered X- and Y-polarization QPSK constellations at 4-dBm input power into each PD for the 32-Gbaud PDM-QPSK mm-wave signal after 80-km SMF-28 transmission in the absence of wireless delivery.

112-GHz radio-frequency (RF) sources. Fig. 3(b) gives the conversion loss of the D-band balanced mixer versus the operating frequency in the scenario of 5-V DC bias, and we can see that the D-band balanced mixer has an average conversion loss of 9.5 dB within the whole D-band. After boost by two parallel EAs with 33-dB gain and DC~50 GHz frequency range, the down-converted 25.5-GHz mm-wave signal is captured by two analog-to-digital (ADC) channels of a 120-GSa/s four-port digital storage oscilloscope (OSC) with 45-GHz electrical bandwidth. The transmitter data can be recovered from the captured 25.5-GHz mm-wave signal after offline DSP, including down conversion, constant-modulus-algorithm (CMA) equalization, carrier recovery, differential decoding, and BER calculation [35]. Fig. 4(a)–(e) give the photos of the whole wireless transmission link, the D-band wireless transmitter end, the D-band wireless receiver end, the X-polarization D-band wireless transmitter end, and the Y-polarization D-band wireless receiver end, respectively.

### 3. Experimental Results for PDM-QPSK Modulated D-Band MIMO Wireless mm-Wave Signal Delivery System

Fig. 5(a) gives the measured BER performance versus the input power into each PD for the 32-Gbaud 137.5-GHz PDM-QPSK mm-wave signal after 80-km SMF-28 transmission in the scenario of no wireless delivery and 0.6-m wireless delivery, respectively. We can see that 0.6-m wireless delivery causes 8-dB power penalty at the BER of  $3.8 \times 10^{-3}$  because of no EAs adopted at the D-band wireless transmitter end. Fig. 5(b) and the two insets in Fig. 5(b) give the captured 25.5-GHz mm-wave signal spectrum as well as the recovered X- and Y-polarization QPSK constellations at 4-dBm input power into each PD for the 32-Gbaud PDM-QPSK mm-wave signal after 80-km SMF-28 transmission in the absence of wireless delivery.

Fig. 6(a) gives the measured BER performance versus the baud rate for the 137.5-GHz PDM-QPSK mm-wave signal after 80-km SMF-28 transmission and 0.6-m wireless delivery at 9-dBm input power into each PD (the output RF power of the PD is -11 dBm at this optical input power). We can see that up to 46 Gbaud corresponds to a BER under  $2 \times 10^{-2}$ . Because the IF output port of this D-band mixer has SMA-connector, which limits the wireless transmission bandwidth, only 46 Gbaud can be realized. Considering that D-band has over 60-GHz bandwidth, the trans-

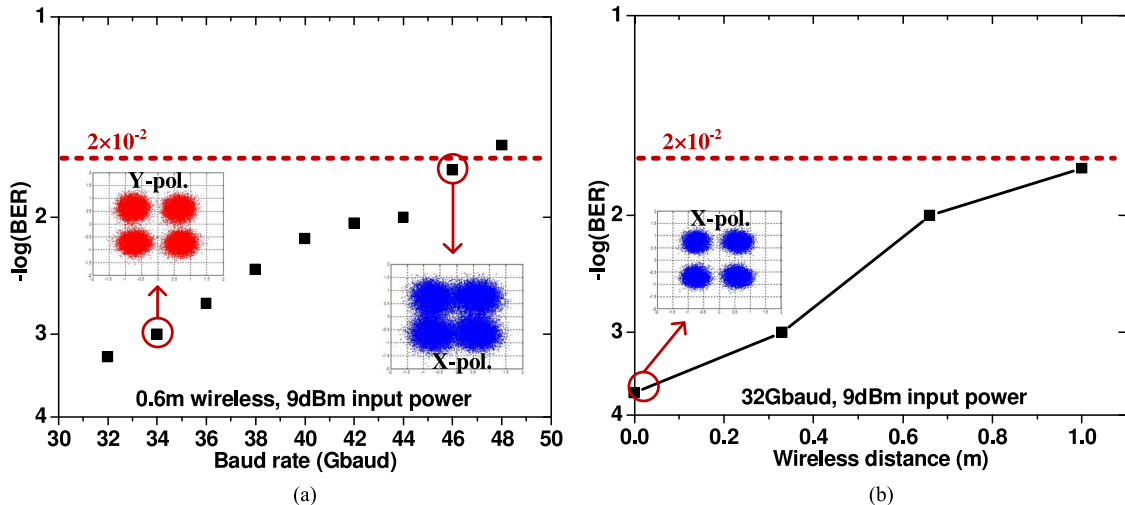


Fig. 6. (a) Measured BER performance versus the baud rate for the 137.5-GHz PDM-QPSK mm-wave signal after 80-km SMF-28 transmission and 0.6-m wireless delivery at 9-dBm input power into each PD. Insets in (a) give the recovered QPSK constellations at 34- and 46-Gbaud baud rates, respectively. (b) Measured BER performance versus the wireless transmission distance for the 32-Gbaud 137.5-GHz PDM-QPSK mm-wave signal after 80-km SMF-28 transmission at 9-dBm input power into each PD. The inset in (b) corresponds to the recovered X-polarization QPSK constellation in the scenario of no wireless delivery.

mission baud rate can be further increased. The two insets in Fig. 6(a) correspond to the recovered QPSK constellations at 34 Gbaud and 46 Gbaud, respectively. Fig. 6(b) gives the measured BER performance versus the wireless transmission distance for the 32-Gbaud 137.5-GHz PDM-QPSK mm-wave signal after 80-km SMF-28 transmission at 9-dBm input power into each PD. The BER increases with the increase of the wireless transmission distance mainly because of the increased wireless path loss, and up to 1-m wireless transmission distance corresponds to a BER under  $2 \times 10^{-2}$ . We think the wireless transmission distance for the 137.5-GHz PDM-QPSK mm-wave signal can be largely extended if a powerful D-band amplifier is applied to both the transmitter end and the receiver end. The inset in Fig. 6(b) corresponds to the recovered X-polarization QPSK constellation in the scenario of no wireless delivery.

#### 4. Experimental Results for PDM-16QAM Modulated D-Band MIMO Wireless mm Wave Signal Delivery System

We also experimentally demonstrate PDM-16QAM modulated D-band MIMO wireless mm-wave signal delivery system. The corresponding experimental setup is quite similar to that given in Fig. 1, except that the I/Q modulator is driven by an 8/16-Gbaud electrical four-level signal with a PRBS length of  $2^{15}-1$  and no fiber transmission is considered. At the wireless mm-wave receiver, cascaded multi-modulus algorithm (CMMA) equalization instead of CMA equalization is used to realize multi-modulus recovery and polarization de-multiplexing of the PDM-16QAM mm-wave signal [35].

Fig. 7(a) gives the measured BER performance versus the input power into each PD for the 8- and 16-Gbaud 137.5-GHz PDM-16QAM mm-wave signal after 10-cm wireless delivery, respectively. We can see that the 8-Gbaud case can reach the HD-FEC threshold of  $3.8 \times 10^{-3}$  while the 16-Gbaud case can reach the SD-FEC threshold of  $2 \times 10^{-2}$ . Fig. 7(b) gives the measured BER performance versus the wireless transmission distance for the 8-Gbaud 137.5-GHz PDM-16QAM mm-wave signal at 10.7-dBm input power into each PD. The BER increases with the increase of the wireless transmission distance mainly because of the increased wireless path loss, and up to 40-cm wireless transmission distance corresponds to a BER under  $2 \times 10^{-2}$ . Similarly, we think

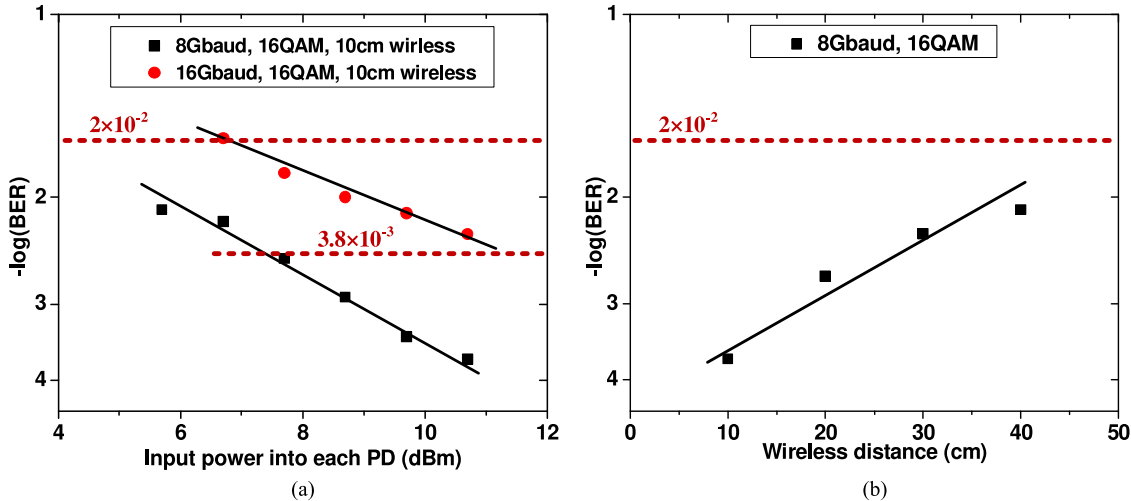


Fig. 7. (a) Measured BER performance versus the input power into each PD for the 8- and 16-Gbaud 137.5-GHz PDM-16QAM mm-wave signal after 10-cm wireless delivery, respectively. (b) Measured BER performance versus the wireless transmission distance for the 8-Gbaud 137.5-GHz mm-wave signal at 10.7-dBm input power into each PD.

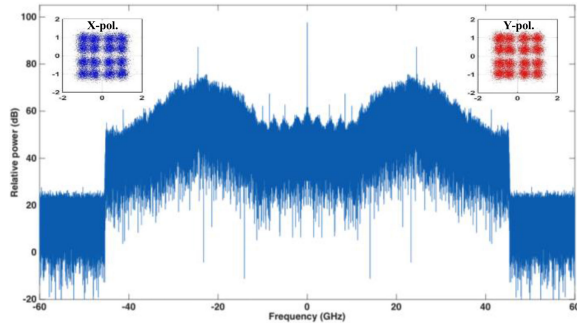


Fig. 8. Captured 25.5-GHz mm-wave signal spectrum. The two insets give the recovered X- and Y-polarization 16QAM constellations.

the wireless transmission distance for the 137.5-GHz PDM-16QAM mm-wave signal can be largely extended if a powerful D-band amplifier is applied to both the transmitter end and the receiver end. Fig. 8 and the two insets in Fig. 8 give the captured 25.5-GHz mm-wave signal spectrum as well as the recovered X- and Y-polarization 16QAM constellations at 10.7-dBm input power into each PD for the 16-Gbaud PDM-16QAM mm-wave signal after 10-cm wireless delivery. Compared to the PDM-QPSK case, the PDM-16QAM case has a lower baud rate, which is because the PDM-16QAM case requires higher-performance components and a higher optical-to-noise ratio (OSNR) compared to the PDM-QPSK case. Compared to the PDM-QPSK case, the PDM-16QAM case also has a relatively short wireless transmission distance, which we think is possibly because the PDM-16QAM signal is more sensitive to the wireless path loss than the PDM-QPSK signal.

## 5. Conclusions

We have experimentally demonstrated an ultra-broadband D-band wireless mm-wave signal delivery system adopting photonics-aided mm-wave generation, wireless MIMO, and high-level vector signal modulation combined with digital heterodyne coherent detection. To the best of our knowledge, we have realized PDM-QPSK wireless mm-wave signal delivery at D-band with the highest baud rate of 46 Gbaud (184 Gbit/s) up to now, and we also realize PDM-16QAM wireless mm-wave signal delivery at D-band with a baud rate of 16 Gbaud (128 Gbit/s).

## References

- [1] K. Kitayama, A. Maruta, and Y. Yoshida, "Digital coherent technology for optical fiber and radio-over-fiber transmission systems," *J. Lightw. Technol.*, vol. 32, no. 20, pp. 3411–3420, Oct. 2014.
- [2] H. J. Song, K. Ajito, Y. Muramoto, A. Wakatsuki, T. Nagatsuma, and N. Kukutsu, "24 Gbit/s data transmission in 300 GHz band for future terahertz communications," *Electron. Lett.*, vol. 48, no. 15, pp. 953–954, 2012.
- [3] S. Koenig *et al.*, "Wireless sub-THz communication system with high data rate," *Nature Photon.*, vol. 7, no. 12, pp. 977–981, 2013.
- [4] D. Zibar *et al.*, "High-capacity wireless signal generation and demodulation in 75- to 110-GHz band employing all optical OFDM," *IEEE Photon. Technol. Lett.*, vol. 23, no. 12, pp. 810–812, Apr. 2011.
- [5] C. W. Chow *et al.*, "100 GHz ultra-wideband (UWB) fiber-to-the-antenna (FTTA) system for in-building and in-home networks," *Opt. Exp.*, vol. 18, no. 2, pp. 473–478, 2010.
- [6] J. Yu *et al.*, "Cost-effective optical millimeter technologies and field demonstrations for very high throughput wireless-over-fiber access systems," *J. Lightw. Technol.*, vol. 28, no. 16, pp. 2376–2397, Aug. 2010.
- [7] Y. Yang, C. Lim, and A. Nirmalathas, "Investigation on transport schemes for efficient high-frequency broadband OFDM transmission in fibre-wireless links," *J. Lightw. Technol.*, vol. 32, no. 2, pp. 267–274, Jan. 2014.
- [8] T. P. McKenna, J. A. Nanzer, and T. R. Clark, "Experimental demonstration of photonic millimeter-wave system for high capacity point-to-point wireless communication," *J. Lightw. Technol.*, vol. 32, no. 20, pp. 3588–3594, Oct. 2014.
- [9] C. Ye, L. Zhang, M. Zhu, J. Yu, S. He, and G. K. Chang, "A bidirectional 60-GHz wireless-over-fiber transport system with centralized local oscillator service delivered to mobile terminals and base stations," *IEEE Photon. Technol. Lett.*, vol. 24, no. 22, pp. 1984–1987, Nov. 2012.
- [10] J. Yu, Z. Jia, L. Yi, Y. Su, G. K. Chang, and T. Wang, "Optical millimeter-wave generation or up-conversion using external modulators," *IEEE Photon. Technol. Lett.*, vol. 18, no. 1, pp. 265–267, Jan. 2006.
- [11] H. J. Song, J. S. Lee, and J. I. Song, "Error-free simultaneous all-optical upconversion of WDM radio-over-fiber signals," *IEEE Photon. Technol. Lett.*, vol. 17, no. 8, pp. 1731–1733, Aug. 2005.
- [12] S. E. Alavi, M. R. K. Soltanian, I. S. Amiri, M. Khalily, A. S. M. Supa'at, and H. Ahmad, "Towards 5G: A photonic based millimeter wave signal generation for applying in 5G access fronthaul," *Sci. Rep.*, vol. 6, 2016, Art. no. 19891.
- [13] A. Kanno *et al.*, "Optical and radio seamless MIMO transmission with 20-Gbaud QPSK," in *Proc. 38th Eur. Conf. Exhib. Opt. Commun.*, Sep. 2012.
- [14] L. Tao *et al.*, "Experimental demonstration of 48-Gb/s PDM-QPSK radio-over-fiber system over 40-GHz mm-wave MIMO wireless transmission," *IEEE Photon. Technol. Lett.*, vol. 24, no. 24, pp. 2276–2279, Dec. 2012.
- [15] J. Yu, X. Li, and N. Chi, "Faster than fiber: Over 100-Gb/s signal delivery in fiber wireless integration system," *Opt. Exp.*, vol. 21, no. 19, pp. 22885–22904, 2013.
- [16] X. Li, Z. Dong, J. Yu, N. Chi, Y. Shao, and G. K. Chang, "Fiber wireless transmission system of 108-Gb/s data over 80-km fiber and 2 × 2 MIMO wireless links at 100 GHz W-band frequency," *Opt. Lett.*, vol. 37, no. 24, pp. 5106–5108, 2012.
- [17] J. Yu, X. Li, J. Zhang, and J. Xiao, "432-Gb/s PDM-16QAM signal wireless delivery at W-band using optical and antenna polarization multiplexing," in *Proc. Eur. Conf. Opt. Commun.*, Sep. 2014.
- [18] X. Li, J. Yu, J. Zhang, Z. Dong, F. Li, and N. Chi, "A 400G optical wireless integration delivery system," *Opt. Exp.*, vol. 21, no. 16, pp. 18812–18819, 2013.
- [19] X. Li, J. Yu, J. Zhang, F. Li, and J. Xiao, "Antenna polarization diversity for 146 Gb/s polarization multiplexing QPSK wireless signal delivery at W-band," in *Proc. Opt. Fiber Commun. Conf. Exhib.*, Mar. 2014.
- [20] X. Pang *et al.*, "100 Gbit/s hybrid optical fiber-wireless link in the W-band (75–110 GHz)," *Opt. Exp.*, vol. 19, no. 25, pp. 24944–24949, 2011.
- [21] X. Li, J. Yu, J. Xiao, Z. Zhang, Y. Xu, and L. Chen, "Field trial of 80-Gb/s PDM-QPSK signal delivery over 300-m wireless distance with MIMO and antenna polarization multiplexing at W-band," in *Proc. Opt. Fiber Commun. Conf. Exhib.*, Mar. 2015.
- [22] X. Li, J. Yu, Z. Dong, J. Zhang, N. Chi, and J. Yu, "Investigation of interference in multiple-input multiple-output wireless transmission at W band for an optical wireless integration system," *Opt. Lett.*, vol. 38, no. 5, pp. 742–744, 2013.
- [23] J. Zhang, J. Yu, N. Chi, Z. Dong, X. Li, and G. K. Chang, "Multichannel 120-Gb/s data transmission over 2 × 2 MIMO fiber-wireless link at W-band," *IEEE Photon. Technol. Lett.*, vol. 25, no. 8, pp. 780–783, Apr. 2013.
- [24] A. Kanno *et al.*, 40 Gb/s W-band (75–110 GHz) 16-QAM radio-over-fiber signal generation and its wireless transmission," in *Proc. 37th Eur. Conf. Exhib. Opt. Commun.*, Sep. 2011.
- [25] X. Li, J. Zhang, J. Xiao, Z. Zhang, Y. Xu, and J. Yu, "W-band 8QAM vector signal generation by MZM-based photonic frequency octupling," *IEEE Photon. Technol. Lett.*, vol. 27, no. 12, pp. 1257–1260, Jun. 2015.
- [26] J. Xiao, Z. Zhang, X. Li, Y. Xu, L. Chen, and J. Yu, "High-frequency photonic vector signal generation employing a single phase modulator," *IEEE Photon. J.*, vol. 7, no. 2, Apr. 2015, Art. no. 7101206.
- [27] C. T. Lin, P. T. Shih, W. J. Jiang, E. Z. Wong, J. J. Chen, and S. Chi, "Photonic vector signal generation at microwave/millimeter-wave bands employing an optical frequency quadrupling scheme," *Opt. Lett.*, vol. 34, no. 14, pp. 2171–2173, 2009.
- [28] M. J. Fice *et al.*, "146-GHz millimeter-wave radio-over-fiber photonic wireless transmission system," *Opt. Exp.*, vol. 20, no. 2, pp. 1769–1774, 2012.
- [29] C. Wang, C. Lin, Q. Chen, B. Lu, X. Deng, and J. Zhang, "A 10-Gbit/s wireless communication link using 16-QAM modulation in 140-GHz band," *IEEE Trans. Microw. Theory Tech.*, vol. 61, no. 7, pp. 2737–2746, Jul. 2013.
- [30] I. Ando, M. Tanio, M. Ito, T. Kuwabara, T. Marumoto, and K. Kunihiro, "Wireless D-band communication up to 60 Gbit/s with 64QAM using GaAs HEMT technology," in *Proc. IEEE Radio Wireless Symp.*, Jan. 2016, pp. 193–195.
- [31] H. Takahashi, A. Hirata, J. Takeuchi, N. Kukutsu, T. Kosugi, and K. Murata, "120-GHz-band 20-Gbit/s transmitter and receiver MMICs using quadrature phase shift keying," in *Proc. 7th Eur. Microw. Integr. Circuits Conf.*, Oct. 2012, pp. 313–316.

- [32] S. Carpenter, Z. He, M. Bao, and H. Zirath, "A highly integrated chipset for 40 Gbps wireless D-band communication based on a 250 nm InP DHBT technology," in *Proc. IEEE Compound Semicond. Integr. Circuit Symp.*, Oct. 2014, pp. 1–4.
- [33] X. Li, Y. Xu, J. Xiao, and J. Yu, "A  $2 \times 2$  MIMO optical wireless system at D-band," in *Proc. Opt. Fiber Commun. Conf. Exhib.*, Mar. 2016.
- [34] X. Li, J. Xiao, and J. Yu, "Long-distance wireless mm-wave signal delivery at W-band," *J. Lightw. Technol.*, vol. 34, no. 2, pp. 661–668, Jan. 2016.
- [35] J. Yu and X. Zhou, "Ultra-high-capacity DWDM transmission system for 100G and beyond," *Commun. Mag.*, vol. 48, pp. S56–S64, 2010.